Aggregation Control of Quantum Dots through Ion-Mediated Hydrogen Bonding Shielding

Jianbo Liu, Xiaohai Yang, Kemin Wang,* Xiaoxiao He, Qing Wang, Jin Huang, and Yan Liu

State Key Laboratory of Chemo/Biosensing and Chemometrics, College of Chemistry and Chemical Engineering, College of Biology, Key Laboratory for Bio-Nanotechnology and Molecular Engineering of Hunan Province, Hunan University, Changsha 410082, P. R. China

ABSTRACT

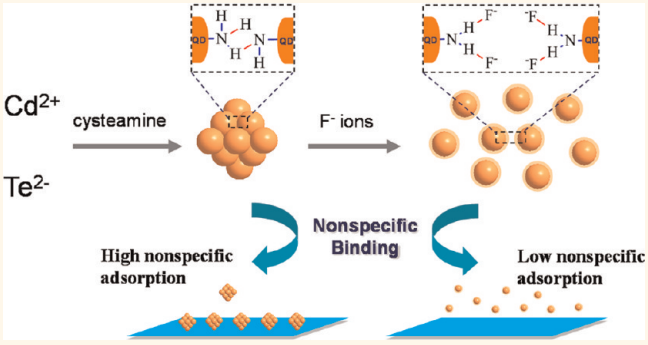

Nanoparticle stabilization against detrimental aggregation is a critical parameter that needs to be well controlled. Herein, we present a facile and rapid ion-mediated dispersing technique that leads to hydrophilic aggregate-free quantum dots (QDs). Because of the shielding of the hydrogen bonds between cysteamine-capped QDs, the presence of F^- ions disassembled the aggregates of QDs and afforded their high colloidal stability. The F^- ions also greatly eliminated the nonspecific adsorption of the QDs on glass slides and cells. Unlike the conventional colloidal stabilized method that requires the use of any organic ligand and/or polymer for the passivation of the nanoparticle surface, the proposed approach adopts the small size and large diffusion coefficient of inorganic ions as dispersant, which offers the disaggregation a fast reaction dynamics and negligible influence on their intrinsic surface functional properties. Therefore, the ion-mediated dispersing strategy showed great potential in chemosensing and biomedical applications.

KEYWORDS: disaggregation · F^- ions · quantum dots · hydrogen bonding · nonspecific adsorption

During recent years, with their flexible processability and unique size-dependent properties, semiconductor quantum dots (QDs) have attracted widespread attentions in the fields of chemosensing and biomedical imaging.[1,2] Although the robust fluorescence signal of QDs provides a highly sensitive response, the selectivity, and reproducibility of QDs-based bioassays can be limited by the tendency of the nanoparticles to agglomerate and nonspecific binding. Therefore, nanoparticle stabilization against detrimental aggregation is a critical parameter that needs to be well controlled,[3] and aggregation-resistant, water-soluble nanoparticles without nonspecific adsorption are desirable, especially in the application of cell imaging and single nanoparticle tracking.[4]

In general, the aggregation usually arose from noncovalent interaction, for example, hydrogen-bonding interaction,[5,6] van der Waals forces,[7] and electrostatic forces[8,9] between the nanoparticles. Thus, the shielding of noncovalent interactions between nanoparticles is one of the approaches to minimize nanoparticle aggregation. The traditional strategies for passivating and stabilizing the surface of nanoparticles are mainly limited to two distinct colloidal processing cases, surface chemical modification[10] and adsorption method.[11] The former strategy usually relied on various zwitterionic molecules,[12,13] or steric hindered macromolecule polymers[14,15] that anchored on the surface of nanoparticles *via* ligand exchange or surface encapsulation. Breus *et al.* has reported the stabilization of fluorescent QDs with zwitterionic d-penicillamine and the resulting QDs exhibited outstanding pH stability and weak nonspecific binding to cells.[16] Polyethylene glycol modified QDs possess nearly neutral surface charges and retain high colloidal stability under various experimental conditions.[17−19] At present, a great deal of amphiphilic polymers,[20−22] phospholipids,[23] dendrimers,[24] and oligomeric ligands[25] have been developed to encapsulate the hydrophobic QDs. However, this approach usually requires the QDs to be chemically tailored and probably modulates the intrinsic composition and structures[26] or surface functional properties of the nanoparticles.[27] Physical adsorption is another commonly used strategy

* Address correspondence to kmwang@hnu.edu.cn.

Received for review February 5, 2012 and accepted May 22, 2012.

Published online May 22, 2012
10.1021/nn300517k

© 2012 American Chemical Society

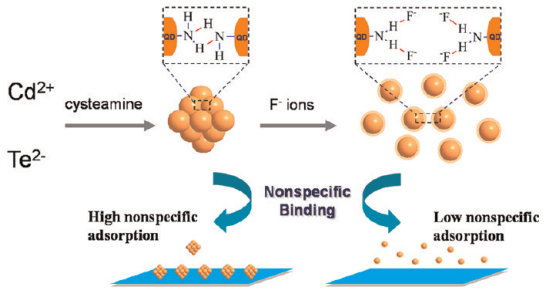

Figure 1. F^- ions mediated hydrogen-bonding shielding for QDs aggregation controlling and significant reduction of nonspecific binding.

for stabilizing nanoparticles. Surfactant[28] and polymers[29] are routinely utilized to passivate on the nanoparticles surface. For instance, the additive bovine serum albumin[30] or Tween[31] in buffer can eliminate the noncovalent interaction between the nanoparticles and efficiently improve the colloidal stability. Obviously, this approach is of simple practice.[32] However, the additive components mostly involve large molecules and probably passivate the active sites of the nanoparticles.[28,33]

It is well-known that the inorganic ions are relatively small matters in the world. We reason the ions as dispersants would exhibit minimal steric exclusion. If the noncovalent interaction between interparticles is modulated by inorganic ions, an ions-mediated dispersing could be established. To demonstrate the feasibility of this design, herein, we present the realization of the concept by F^- ions mediated hydrogen-bonding shielding for disaggregation of fluorescent QDs. Ions-triggered reversible disassembly that resulted in fluorescence recovery of QDs for analytical detection has been performed in our previous work.[34] However, until now, we are unaware of any studies which have examined the inorganic ions as dispersants for nanoparticle aggregation controlling. The aim of this work was to propose an ions-mediated colloidal dispersing methodology for biomedical imaging. F^- ions, with their strong electronegativity, show strong H-binding capability,[35] and thus can act as hydrogen-bonding acceptors to mediate the self-assembly of various inorganic and organic nanomaterials.[34,36,37] Here, the conditions of our proposed approach comprise F^- ions triggered hydrogen-bonding shielding for QD aggregates. As illustrated in Figure 1, the simultaneous addition of F^- ions into cysteamine-capped QD aggregates suspension and the substitution of hydrogen bonds between interparticles resulted in monodisperse individual QDs that formed extremely stable colloidal water dispersions. Meanwhile, the presence of F^- ions also greatly eliminated the nonspecific adsorption of the QDs on glass slides and cell. The most remarkable fact concerning the nanoparticle aggregation control is that this approach involves neither any surface modification of charged/steric hindered ligands nor any physically adsorption of surfactants or polymers. Taking advantage of small size and strong electronegativity of F^- ion, this method provides a fast disassemble dynamics and minimal effect on the intrinsic surface properties of the nanoparticles.

RESULTS AND DISCUSSION

Characterization of the Disaggregation. Here, F^- ions mediated disaggregation of cysteamine-capped QDs was demonstrated. The reason cysteamine was chosen as the ligand of QDs for this design was that cysteamine is one of the most important chelating ligands in coordination chemistry and binds preferentially to soft metal ions.[38] Besides, the terminal amino group on the surface of nanoparticles can be conjugated with nearly all protein or peptide molecules as well as a host of other macromolecules through coupling chemical reactions because the modification of amines proceeds by acylation or alkylation. Therefore, cysteamine is being intensively studied as a coating material for the molecular imaging of nanoparticles, and cysteamine-capped QDs show promising biological applications.[39] The fluorescent cysteamine-capped CdTe QDs were fabricated *via* a modified aqueous synthetic procedure.[40] The freshly produced H_2Te gas was introduced into the cysteamine-stabilized Cd precursor solution, which resulted in the nucleation of CdTe QDs. The QDs gradually grew up under reflux conditions. During the growth process or storage, aggregation usually occurred for the QDs around neutral pH. Cysteamine-capped QDs are colloidally unstable. This was because the terminal amino groups on the surface of cysteamine-capped QDs appeared to be deprotonated and interparticle NH—N hydrogen bonds between neighboring QDs formed.[34,38,41] In general, for the QDs application in biomedical fields, the QD surface should meet the following criteria: (i) good colloidal stability without aggregation; (ii) minimal hydrodynamic size;[42] (iii) minimal nonspecific binding for specific targeting; and (iv) flexibility for allowing simple conjugations.[41] Thus, good colloidal stability without aggregation is the precondition of further bioconjugation and biomedical application.

F^- ions, widely existing in nature, play great important roles in environmental, industrial, and biological processes.[43,44] Because of their strong electronegativity, F^- ions can act as hydrogen-bonding acceptors to mediate the reversible self-assembly of nanoparticles.[34,45,46] Here, the ion-mediated dispersion of QD aggregates was performed at neutral pH. Cysteamine-capped CdTe QDs with a fluorescence peak at 597 nm were utilized (Supporting Information, Figure S1). At room temperature, F^- ions solution with identical pH value was gradually added into the suspension of QDs aggregates under gentle stirring. It was observed that

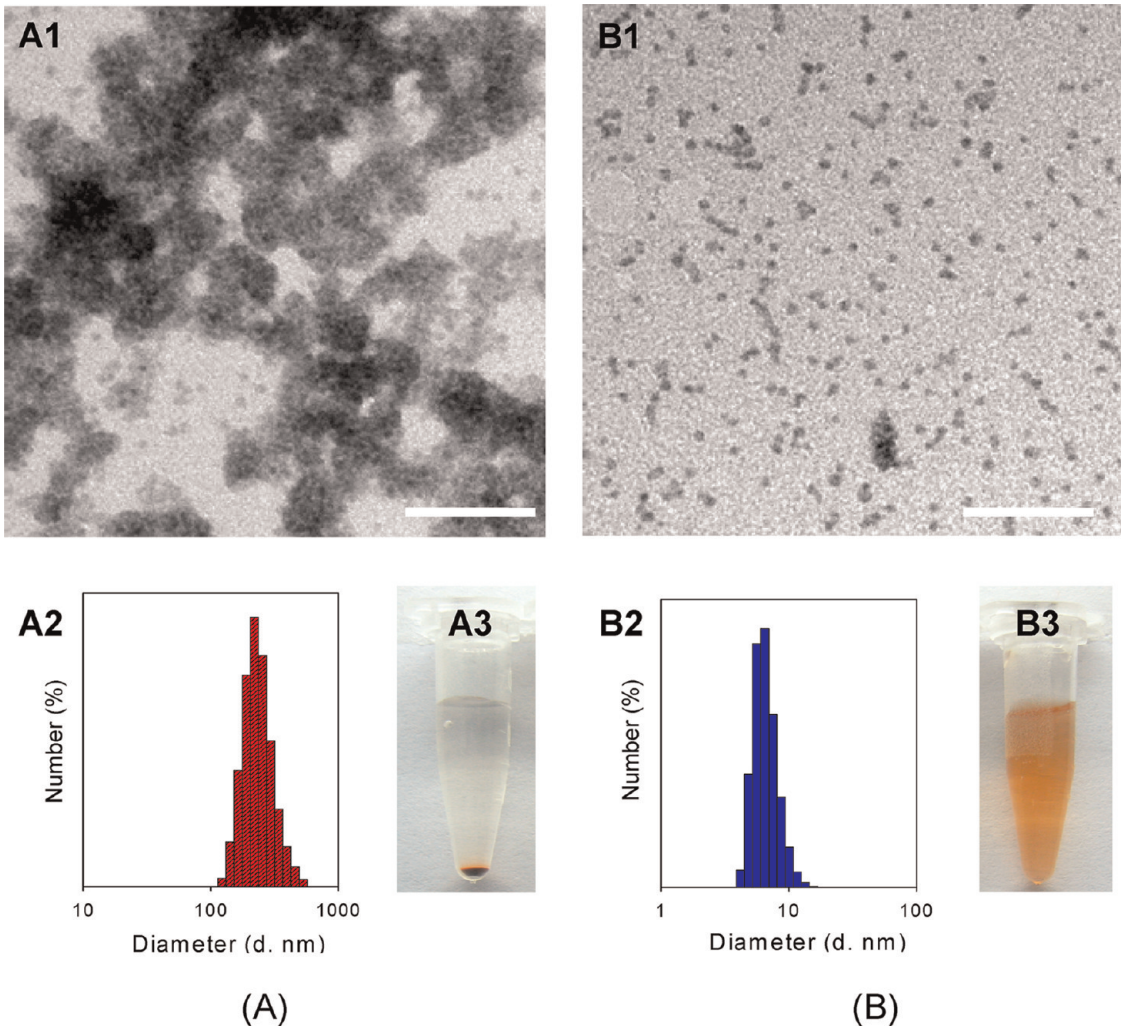

Figure 2. TEM images (A1 and B1), hydrodynamic diameters (A2 and B2), and photographs of cysteamine-capped QDs (A3 and B3) before (A) and after (B) addition of F^- ions. Bar: 50 nm. The concentrations of QDs and F^- ions were ~10 μM and 100 mM, respectively. The experiment was performed in pH 7.0 aqueous solution at room temperature.

the QD suspension quickly became disperse, even without any ultrasonic process. The obtained aqueous QD solutions demonstrated extremely high colloidal stability and no precipitations were observed for more than two years of storage. To demonstrate the ions-triggered-disaggregation behavior, a TEM imaging experiment was performed. As illustrated in Figure 2, TEM results revealed that the initial cysteamine-capped CdTe QDs were highly aggregated. The EDS result validated the composition of cysteamine-capped CdTe QDs, and HRTEM further disclosed that the QD aggregates were closely compacted (Supporting Information, Figure S2). In contrast, finely monodisperse QDs were formed after introduction of F^- ions. The hydrodynamic diameters were further determined by dynamic light scattering (DLS). In agreement with the TEM results, the hydrodynamic diameters of the particles decreased from 242.6 $\pm$ 71.7 nm to 6.7 $\pm$ 1.6 nm after the addition of F^- ions, providing a strong indication of the disintegration. A convenient criteria for aggregation-free QDs is that their hydrodynamic diameter should be less than twice of their primary size.[4] Here, their primary size was *ca.* 3.8 nm determined by HRTEM (Supporting Information, Figure S1), thus it implied that the dispersed QDs turned out to be individual monomeric state. The disaggregation was accompanied by the fluorescence recovery of the QDs (Supporting Information, Figure S3), which was consistent with that reported in our previous work.[34] Fluorescence self-quenching occurred as the aggregation of fluorescent QDs.[47−49] In a reversible process, the disaggregation resulted in the recovery of the quenched fluorescence.

The disassembly of QDs aggregates depended on the concentration of F^- ion. As shown in Supporting Information, Figure S4(A1), hydrodynamic diameters of the QD aggregates (~10 μM) gradually decreased as the F^- ions solution was gradually added. Further experiments revealed that the extent of aggregation could vary with the concentration of QDs and F^- ions. As shown in Supporting Information, Figure S4(A1−A5), the changes of QD aggregates sizes at different initial

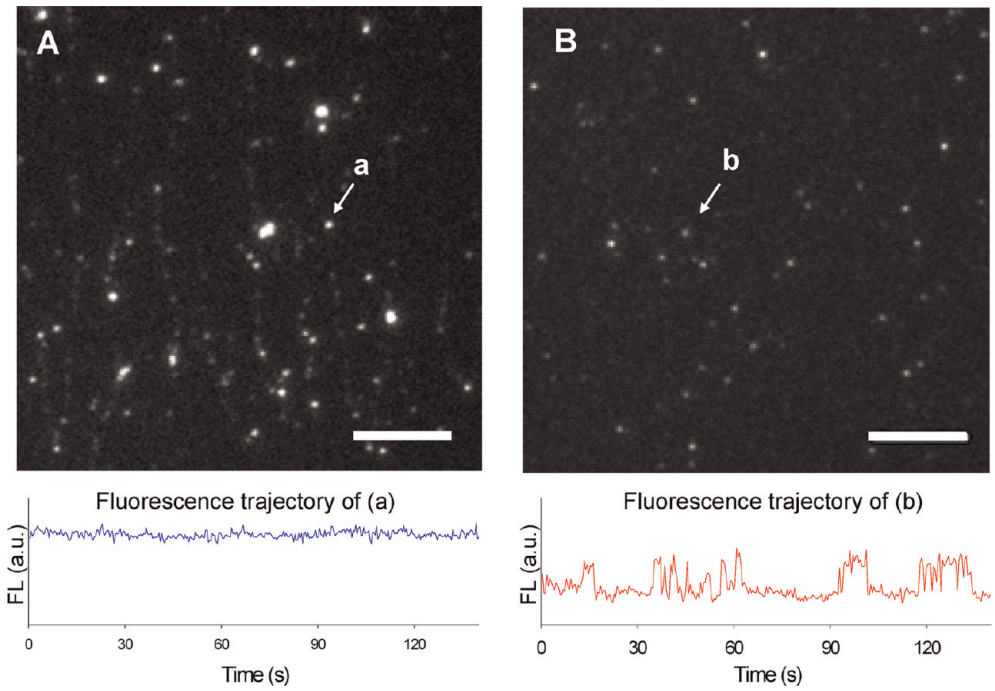

Figure 3. Fluorescence imaging of QDs in the absence of (A) and in the presence of F^- ions (B); bar, 5 μm. Bottom: representative time trajectories of single fluorescent spot. The initial concentrations of QDs and F^- ions were ~10 μM and 100 mM, respectively. The experiment was performed in pH 7.0 aqueous solution at room temperature.

concentrations upon the introduction of F^- ions were investigated. Their sizes all gradually decreased as F^- ions solution was gradually added. The larger the concentration of QD aggregate was, the more F^- ions should have been added. The quantitative concentration dependent relationship of QD aggregates with F^- ions that completely disassemble the aggregates is plotted in Supporting Information, Figure 4(B). The results showed that the amount of F^- ions added to completely disassemble the aggregates was linearly correlated to that of the QD aggregates. However, excessive F^- ions addition may also lead to aggregation again because of the screening of the electrostatic repulsion between particles at high salt concentration.

Single Nanoparticle Imaging. The fluorescence emission of the single fluorophore is usually characteristically intermittent.[50] It means that for individual QDs, its emitter behaves as being intermittent and the bright/dim intervals randomly follow each other. In contrast, for ensemble aggregates, this intermittent behavior is always hidden because the fluctuations of an individual object are not synchronized.[51,52] Thus their intermittent property is generally considered as a clue to distinguish a single QD from an aggregate. To further validate the different dispersion states of the QDs, single nanoparticle fluorescence imaging was performed. The experiment was conducted on a total internal reflection fluorescence (TIRF) microscope. The QDs were diluted and then spin-coated on the glass surface. Figure 3 shows the fluorescence imaging of different QD suspensions. It was demonstrated that fluorescent spots exhibited uneven fluorescence intensity for cysteamine-capped QD aggregates. However, after addition of F^- ions, their fluorescence intensity became evenly distributed. Time trajectories inserted in Figure 3 were obtained for a single fluorescence spot. It displayed a continuum of intensity level for QDs in absence of F^- ions. In contrast, after the introduction of F^- ions, a discrete intensity level can be observed for QDs. Thus, the intermittent imaging results further confirmed that after the addition of F^- ions, the QDs are primarily well-dispersed at single-particle level.

Mechanism of Aggregation Controlling. As mentioned above, we believe the occurrence of aggregation was originated from interparticle hydrogen bonding, thus the disassembly of QD aggregates may involve the hydrogen-bonding shielding. Our data revealed that the surface potentials of nanoparticles had no obvious change before and after the addition of F^- ions (Supporting Information, Figure S5). The results also suggested the disaggregation was not a result from the repulsion of an electrostatic force between interparticles. It is well-known that F^- ions with the strongest electronegativity could establish strong hydrogen bonding. Therefore, it was reasoned that the disassembly of QD aggregates was attributed to the NH—F formation substituting for NH—N hydrogen bonding (Figure 1).[34] This was confirmed by the ^{1}H NMR titration experiments (Figure 4A). The chemical shift of the α-methylene protons of cysteamine was moved to a high field upon gradual addition of F^- to the

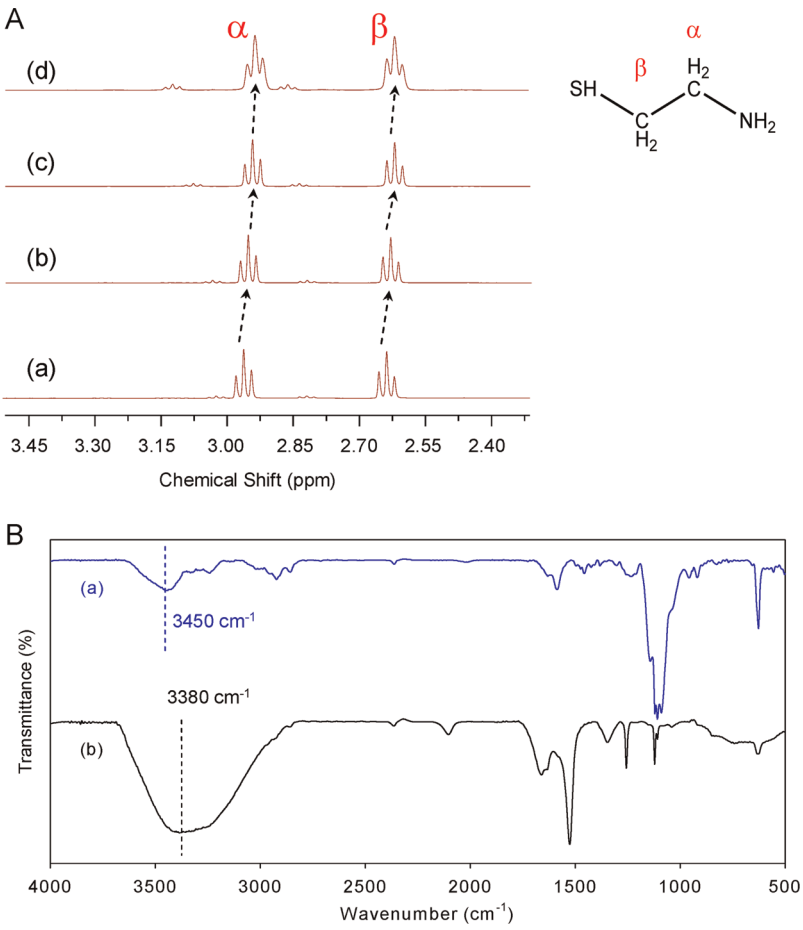

Figure 4. (A) ^{1}H NMR spectra of cysteamine-capped QDs aggregates (10 μM) on the addition of F^- ions in D_2O. The concentrations of F^- ions were a (0), b (20 mM), c (60 mM), d (100 mM), respectively. Primary amine groups of cysteamine have not been observed in ^{1}H NMR spectra, because of fast proton transformation. (B) FTIR spectra of QDs aggregates (10 μM) powders in the (1) absence and (2) presence of F^- ions (100 mM). Samples of QDs were dehydrated by vacuum freeze-drying before analysis.

cysteamine-capped QDs solution of D_2O. The addition of F^- ions to QDs caused the progressive chemical shift to move from δ 2.96 ppm to δ 2.93 ppm. This is because F^- ions cause a deshielding of NH protons due to NH—F hydrogen-bonding formation. Upon formation of the hydrogen bonding, the N—H bonds become more polarized, which increases the electron density on the nitrogen atom. Consequently, the electron density of the adjacent methylene group is increased because of an inductive effect. Thus, the protons on the methylene group are deshielded and their chemical shifts move to high field.[53] As further evident in FTIR spectra (Figure 4B), the stretching peak broadening and shift from 3452 to 3345 cm^{-1} (νs NH_2) of the QDs upon addition of F^- ions indicated strong hydrogen-bonding formation.[34] Therefore, it is believed that the cysteamine-capped QD aggregates disassemble due to F^- ions mediated hydrogen-bonding shielding. This was consistent with the results reported in literature for a supramolecular gel, where the NH bond in the amide group interacted with F^- ions *via* hydrogen bonding resulting in a disruption of the gel state.[37]

The hydrogen-bonding-prompted disaggregation should be a pH dependent process. As pH decreased, a gradual decrease in the hydrodynamic diameter of the QDs aggregates was observed (Supporting Information, Figure S6), suggesting the occurrence of disaggregation. In addition, hydrogen-bonds formation is thermodynamically favored, and the disaggregation process could be temperature dependent. As the temperature increased from 0 to 60 °C, the hydrodynamic diameter of the QDs aggregates gradually decreased (Figure S6). Generally, NH—N hydrogen bonding with weak bonding energy was more sensitive to pH value and environment temperature than strong NH—F hydrogen bonding. Thus, the disaggregation occurrence as pH decreased or temperature increased resulted from NH—N hydrogen-bond breaking. However, the QD aggregate sizes always became small after the addition of F^- ions. Thus, it was concluded that F^- ions still showed dispersion ability to QD aggregates at different pH and temperature.

As compared with the conventional dispersion method, the F^- ion-mediated dispersion shows some

novel features. First, the ions possess relatively small angstrom-level size, which allows them to penetrate into an even narrow space to disassemble severe aggregates. Here, cysteamine was chosen as the ligand of QDs for this design because cysteamine can provide a short interparticle distance between neighboring QDs. To examine whether the F^- ions can penetrate into the pores of the QD aggregates or not, we calculated the interparticle distance between neighboring QDs using a 3D chemical structure model (Figure 5). The spatial distance is estimated to be *ca.* 8.61 Å and perhaps, only small ions, for example, F^- ions (ion diameter at 2.6 Å)[54] can enter into the rigorous aggregates. All halide ions were employed to dispersing the QD aggregates. It was demonstrated that the cysteamine-capped QD aggregates cannot be disassembled by the anions tested other than F^- ions (Supporting Information, Figure S7). Even a 1.0 M high concentration of chloride ion did not exert similar results to the QDs as that of the F^- ions. Meanwhile, our experiments also showed that the aggregates cannot be disassembled by any surfactants, such as EDTA and CTAB (Figure S7).

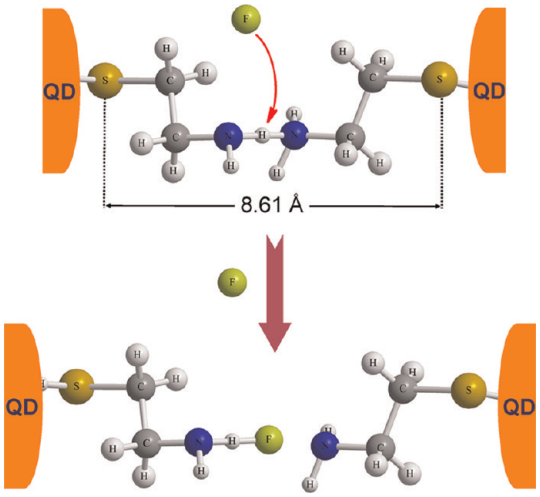

Figure 5. Mechanism diagraph of F^- ions-triggered dispersion of cysteamine-capped QD aggregates; estimation calculation of the interparticle distance for QD aggregates using 3D chemical structure model.

Recently, the adsorption on porous materials is one of the most promising processes for F^- ions removal.[55,56] Novel adsorbents for F^- ions removal include China clay, calcite, hydroxyapatite, amorphous alumina, and so on.[57,58] Similar with that of the adsorbents, the QD aggregates also possess porous structure that allows small size F^- ions to enter. The F^- ions exhibit a large diffusion coefficient of 14.75 $cm^2\ s^{-1}$,[59] which provides a fast reaction dynamics. Therefore, the QDs aggregates can be disassembled immediately upon the addition of F^- ions. This is a great benefit for heterogeneous surface analysis, including biochip and cell imaging, because of the low reaction dynamics for solid–liquid interface.

The most appealing feature of the ion-mediated dispersion method is that this approach does not change the surface functional properties of the nanoparticles and the cysteamine-capped QDs retained their intrinsic function for their applications in biological/chemical fields. To demonstrate their efficient bioconjugation, the binding of QDs to agarose microbeads through a biotin–streptavidin system was conducted (Supporting Information, Figure S8). The fluorescence of QDs that modified on the agarose microbeads was characterized by fluorescent microscopy. As displayed in Figure 6, the agarose microbeads modified with the F^- ions-triggered monodisperse QDs showed bright fluorescence. However, the microbeads modified with aggregated QDs showed dim fluorescence. It was possible that two factors resulted in the distinguished fluorescence intensity. On the one hand, as discussed above, the fluorescence recovery of QDs was accompanied by the disaggregation process,

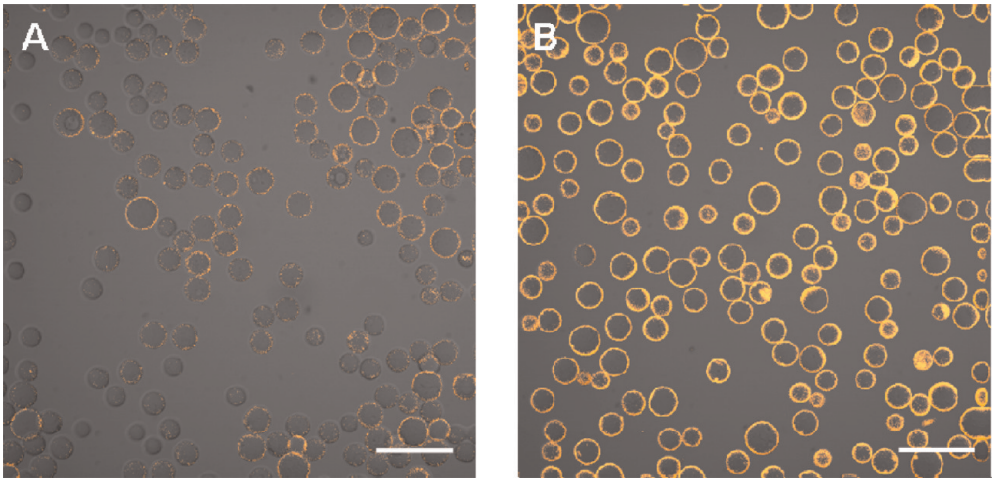

Figure 6. Fluorescent imaging of agarose microbeads modified with QDs through the biotin–streptavidin system. The QDs were biotinylated and then cultured with streptavidin–agarose microbeads. QDs suspension (A) in the absence of and (B) in the presence of F^- ions. Scale bar: 100 μm.

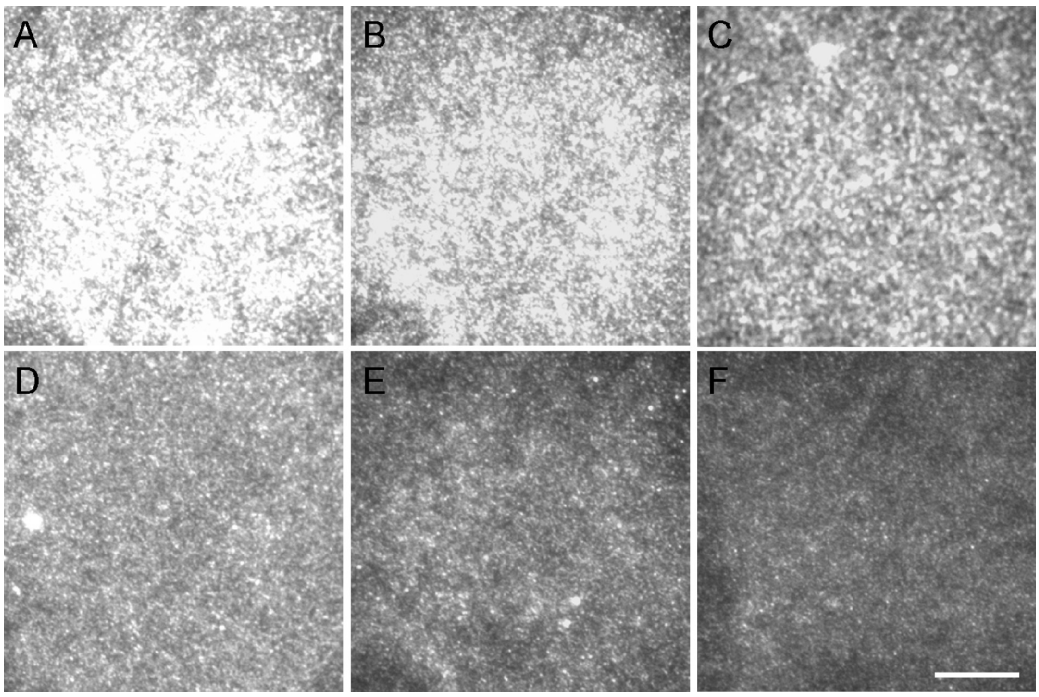

Figure 7. Fluorescence imaging of QDs (0.1 μM) with different concentrations of F^- ions deposited on plasma-cleaned glass surfaces. F^- ions concentrations: (A) 0, (B) 0.2, (C) 0.4, (D) 0.6, (E) 0.8, (F) 1.0 mM. Scale bar: 20 μm.

which would offer the QDs functionalized microbeads fluorescence enhancement. On the other hand, a higher efficient bioconjugation for disaggregated QDs happened. The amount of QDs modified with microbeads was quantified by the potentiometric stripping voltammetry of Cd(II) after the dissolution of the CdTe tags with HNO_3 (Supporting Information, Figure S9). It was observed that the amount of Cd(II) for monodisperse QDs modified microbeads was about 4.3 times than that of QD aggregates modified microbeads. We inferred that after disaggregation of QDs in the presence of F^- ions, the steric hindrance was greatly eliminated, which thus greatly improved the bioconjugation efficiency. Thus, taking advantage of the small size of F^- ions, the ion-mediated dispersing method showed negligible influence on their intrinsic surface functional properties, which showed great promise for biological assay and fluorescent imaging.

Nonspecific Binding Experiments. The fluorescent QDs are widely used in the field of biochips, cell imaging, and bioassay. One major problem is that QD probes tend to be sticky and often bind nonspecifically to glass slides, cellular membranes, and extracellular matrix materials.[41,60] This nonspecific binding problem causes a high level of background fluorescence that decreases the signal-to-noise ratio and limits tagging specificity and detection sensitivity. Hence, preventing nonspecific adsorption has attracted great attention. Ions-mediated hydrogen-bonding shielding may be utilized to reduce nonspecific adsorption. Here, nonspecific binding of cysteamine-capped QDs on glass slides before and after the addition of F^- ions was investigated. As illustrated in Figure 7, the QD aggregates largely adhered to glass surfaces and exhibited intensive fluorescence signal. However, in the presence of F^- ions, the nonspecific adsorption was greatly inhibited. The nonspecific adsorption was mostly originated from the noncovalent interactions, for example, NH—O hydrogen bonding between amino groups of the QDs and hydroxyl groups of glass. We inferred that the strong hydrogen bonding between F^- ions and amino groups blocked the hydrogen-bonding interaction, which thus greatly inhibited the nonspecific adsorption (Supporting Information, Figure S10). In addition, the nonspecific adsorption of the QDs on the cell was further investigated. As presented in Figure 8, a significant nonspecific interaction of the QD aggregates with the cell membrane appeared as remarkable fluorescent spots. *Z*-axis scanning imaging by fluorescent confocal microscopy indicated that the QDs were mostly adsorbed surrounding the cell and part of them may be internalized (Supporting Information, Figure S11). In contrast, after the addition of F^- ions, a very slight, nonspecific interaction between the QDs and the cell membrane was observed. As explained in the case of glass slides, we assumed F^- ions-mediated hydrogen-bonding shielding blocked the hydrogen-bonding interaction between amino groups of the QDs and the surface functional groups of the cell. Here, the adopted QD and maximal F^- ion concentrations were 0.10 μM and 1.0 mM, respectively, and F^- ions showed good capability to disassemble the aggregates in this concentration region (Supporting Information, Figure S4).

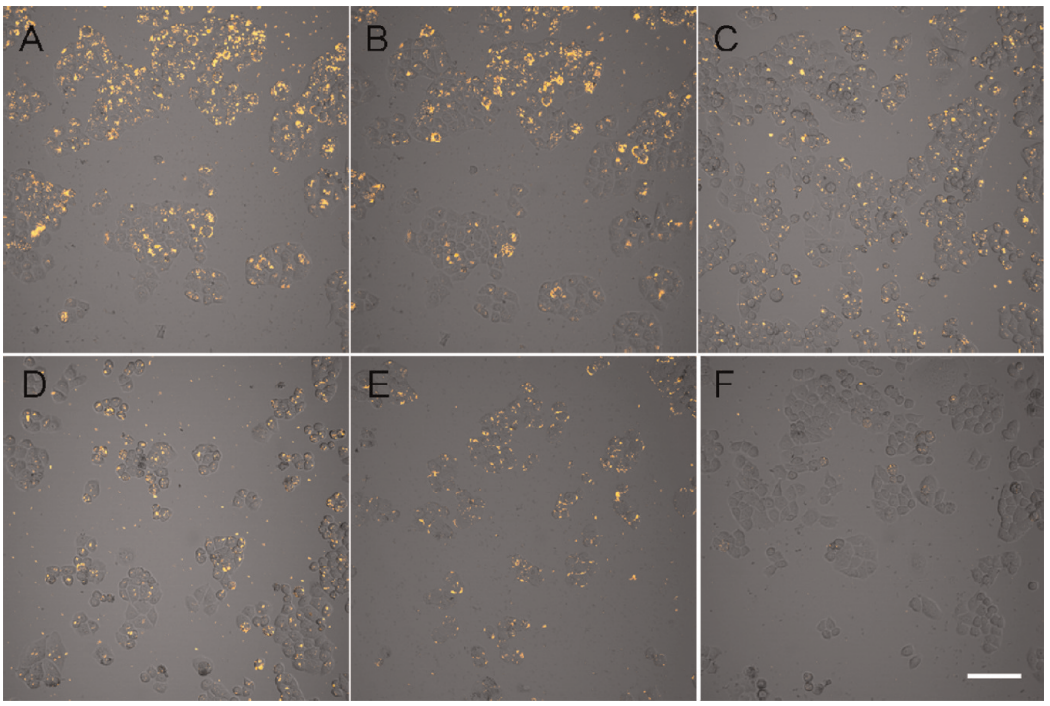

Figure 8. Cell images of Hela cells cultured with QDs (0.1 μM) with different concentration of F^- ions for 30 min. The F^- ions concentrations: (A) 0, (B) 0.2, (C) 0.4, (D) 0.6, (E) 0.8, (F) 1.0 mM. Scale bar:100 μm.

The reason that the low concentration was adopted is because a high dose of inorganic fluoride (>10 mM) usually results in statistically significant cell death.[61] Fortunately, the dose adopted in our cell experiment was less than the lethal concentration, and no morphologic change of cells was observed. Thereby, the F^- stimulated dispersing QDs with a weak nonspecific binding is of practical importance for cellular labeling and fluorescence imaging applications.

CONCLUSION

In conclusion, we proposed a facile ion-mediated aggregation control method for cysteamine-capped QDs. Because of the shielding of the hydrogen bonds between cysteamine-capped QDs, the presence of F^- ions disassembled the aggregates of the QDs and afforded their highly colloidal stability. More specifically, nonspecific adsorption of QDs on glass and cell was greatly eliminated. The approach provides a new aggregation control mechanism for nanoparticles. Taking advantage of the ions of small size, this method provides a fast disassemble dynamics and minimal effect on the surface functional properties of nanoparticles. The results would benefit the further applications of QDs for analytical detection and fluorescence imaging. We hope that the concept developed in this study may be expanded for improving colloidal stability of other nanoparticles.

MATERIALS AND METHODS

Materials. Cadmium perchlorate hexahydrate ($Cd(ClO_4)_2 \cdot 6H_2O$, 99%) was purchased from Acros Organics. Cysteamine (95%) and biotin *N*-hydroxysuccinimide (Biotin-NHS) were purchased from Sigma-Aldrich. Telluride power and sodium fluoride (NaF, ≥98.0%) were purchased from Sinopharm. Streptavidin–agarose hydrogel microbeads (Sepharose, agarose 6%, ~34 μm) were purchased from GE Healthcare. Unless otherwise noted, all reagent-grade chemicals were used as received. pH of the solution was adjusted by 0.1 M NaOH or HCl.

Characterization. Steady-state fluorescence measurements were performed on a Hitachi F-7000 fluorescence spectrophotometer with excitation wavelength at 400 nm. Absorption spectra were recorded on a UV–vis 1601 Shimadzu spectrophotometer. FTIR spectra of KBr powder-pressed pellets were recorded on a Bruker Tensor 27 spectrophotometer scanning from 4000 to 400 cm^{-1}. Dynamic light scatter (DLS) experiments were carried out in a Malvern Nano-ZS system equipped with a He–Ne laser working at 633 nm to examine the hydrodynamic diameter (number-weighted mean diameter) and zeta potentials of QDs aggregates. Transmission electron microscopy (TEM) and energy dispersive spectrograph (EDS) was performed on JEOM 3010 microscopy (JEOL). TEM samples were prepared by spin coating a thin layer of QDs resist onto a carbon-coated copper grid substrate, which was then baked with an infrared lamp. ^1H NMR spectra were recorded on a 400 MHz spectrometer (Varian Inova-400). NMR titration experiments were carried out in D_2O at 298 K.

Synthesis of Cysteamine-Capped CdTe QDs. CdTe QDs stabilized by cysteamine were prepared in water, as described previously.[40] CdTe QDs with fluorescence peak at 597 nm ($\Phi \approx 15\%$) were used. The mole concentration of CdTe QDs was determined as a procedure reported by Peng *et al.*[62]

Single Nanoparticle Imaging. Single nanoparticle fluorescence measurements were performed on total internal reflection fluorescence (TIRF) microscope (Nikon, TE-2000U inverted microscope) with a 60× TIRF objective. The fluorescence image

was collected through Cy3 fluorescent channel (emission bandpass 593 ± 40 nm, Semrock) and captured on C9100-13 EMCCD (Hamamatsu). Integration times of 100 ms per frame were used to obtain 256 × 256 pixels. The samples were excited with a typical power density of *ca.* 2.5 $W \cdot cm^{-2}$ from a 532 nm solid state laser (Mellus Griot, Green Solid State). Intensity time trajectories were obtained by a sequence of imaging movie. The fluorescent imaging data were analyzed by SimplePCI 6.5 (Hamamatsu). Before observation, the QDs were diluted to a certain concentration where the white spots are distributed separately when projected to the EMCCD chip. The QDs solution of 5 μL was spin-coated onto the well-cleaned glass slide (Fisher). All measurements were performed in a dark compartment at room temperature.

Fluorescent Imaging of Microbeads. The biotinylation of cysteamine-capped QDs: 1 $mg \cdot mL^{-1}$ solution of biotin-NHS was prepared in DMSO. Biotin−NHS (5 mM) was mixed with 1.5 μM QDs and incubated on a rotator for 4 h at room temperature. The biotinylated QDs were collected after centrifugation for 10 min at 10000 rpm. The biotinylated QDs were then incubated with streptavidin−agarose hydrogel microbeads. After incubation for 30 min the microbeads were collected after centrifugation for 30 s at 500 rpm. The QD−labeled microbeads were washed and then analyzed on the confocal laser scanning microscopy. To quantify the amount of QDs modified with agarose microbeads, the microbeads were first dissolved in nitric acid. Cd(II) concentration was then measured with potentiometric stripping voltammetry on an electrochemical workstation (model CHI-660, Shanghai Chenhua Apparatus Company, China). The working electrode is a form of thin mercury film on glassy carbon. A calomel electrode and a platinum wire were used as the reference and counter electrode, respectively. Electrodeposition potential and deposition time were −1.2 V and 180 s, respectively. After a 30 s rest period (without stirring), stripping was performed by scanning the potential from −1.2 to −0.3 V.

Nonspecific Adsorption Experiments. The nonspecific adsoption of the cysteamine-capped QDs after the addition of F^- ions to the glass slides was studied. An aliquot of 200 μL of QD suspensions (0.1 μM) with different concentrations of F^- ions (0−1.0 mM) was deposited onto the glass slide and allowed to react for 10 min. The slides were imaged using a TIRF microscope with a 60× objective.

The nonspecific adsorption of QDs on the cells was performed as following. Hela cells were cultured in RPMI 1640 medium supplemented with 10% FBS and 100 $IU \cdot mL^{-1}$ penicillin−streptomycin. Cells were seeded on 35-mm glass bottom dishes (MatTek, Ashland, MA) and cultured at 37 °C under 5% humidified CO_2 for 24 h. Hela cells were plated in 35-mm glass bottom culture dishes, grown to 80% confluency for 24 h at 37 °C, and washed three times with prewarmed phosphate-buffered saline (PBS). The culture medium was then replaced with PBS. A suspension of QDs (0.1 μM) with different concentrations of F^- ions (0−1.0 mM) was added into the dishes, respectively. After incubation for 30 min at 37 °C, the cells were washed with PBS buffer. The cell imaging was conducted with a confocal laser scanning microscopy setup consisting of a heated specimen holder and an Olympus IX-70 inverted microscopy with an Olympus FluoView 500 confocal scanning system.

Conflict of Interest: The authors declare no competing financial interest.

Acknowledgment. This work was supported by the National Natural Science Foundation of China (90606003, 21190041, 21190044, 21175035), National Basic Research Program (2011CB911002), International Science & Technology Cooperation Program of China (2010DFB30300), Program for New Century Excellent Talents in University (NCET-09-0338), and Hunan Provincial Natural Science Foundation of China (10JJ7002).

Supporting Information Available: Absorption, fluorescent spectra, TEM imaging, and EDS analysis of CdTe QDs; effects of concentration, pH, and temperature, zeta potentials, potentiometric stripping voltammetry. This material is available free of charge *via* the Internet at http://pubs.acs.org.

REFERENCES AND NOTES

1. Jin, Y.; Gao, X. Plasmonic Fluorescent Quantum Dots. *Nat. Nanotechnol.* **2009**, *4*, 571–576.
2. Hildebrandt, N. Biofunctional Quantum Dots: Controlled Conjugation for Multiplexed Biosensors. *ACS Nano* **2011**, *5*, 5286–5290.
3. Vuluga, D.; Legros, J.; Crousse, B.; Bonnet-Delpon, D. Solubility Switch of Gold Nanoparticles through Hydrogen Bond Association. *Chem. Commun.* **2008**, *40*, 4954–4955.
4. Moon, J.; Choi, K. S.; Kim, B.; Yoon, K. H.; Seong, T. Y.; Woo, K. Aggregation-free Process for Functional CdSe/CdS Core/Shell Quantum Dots. *J. Phys. Chem. C* **2009**, *113*, 7114–7119.
5. Mandal, S.; Gole, A.; Lala, N.; Gonnade, R.; Ganvir, V.; Sastry, M. Studies on the Reversible Aggregation of Cysteine-Capped Colloidal Silver Particles Interconnected *via* Hydrogen Bonds. *Langmuir* **2001**, *17*, 6262–6268.
6. Starck, P.; Ducker, W. A. Simple Method for Controlled Association of Colloidal-Particle Mixtures Using pH-Dependent Hydrogen Bonding. *Langmuir* **2009**, *25*, 2114–2120.
7. Radhakrishnan, C.; Lo, M. K. F.; Knobler, C. M.; Garcia-Garibay, M. A.; Monbouquette, H. G. Capping-Ligand Effect on the Stability of CdSe Quantum Dot Langmuir Monolayers. *Langmuir* **2011**, *27*, 2099–2103.
8. Sven, H. B.; Michal, B. Stabilization of Aqueous Colloidal Dispersions: Electrostatic and Steric Forces. In *Encyclopedia of Surface and Colloid Science*, 2nd ed.; Taylor & Francis: Boca Raton, FL, 2007; pp 5765−5774.
9. Halpert, J. E.; Tischler, J. R.; Nair, G.; Walker, B. J.; Liu, W.; Bulovic, V.; Bawendi, M. G. Electrostatic Formation of Quantum Dot/J-Aggregate FRET Pairs in Solution. *J. Phys. Chem. C* **2009**, *113*, 9986–9992.
10. Estephan, Z. G.; Jaber, J. A.; Schlenoff, J. B. Zwitterion-Stabilized Silica Nanoparticles: Toward Nonstick Nano. *Langmuir* **2010**, *26*, 16884–16889.
11. Moskovits, M.; Vlckov, B. Adsorbate-Induced Silver Nanoparticle Aggregation Kinetics. *J. Phys. Chem. B* **2005**, *109*, 14755–14758.
12. Rouhana, L. L.; Jaber, J. A.; Schlenoff, J. B. Aggregation-Resistant Water-Soluble Gold Nanoparticles. *Langmuir* **2007**, *23*, 12799–12801.
13. Ding, Y.; Xia, X. H.; Zhai, H. S. Reversible Assembly and Disassembly of Gold Nanoparticles Directed by a Zwitterionic Polymer. *Chem.—Eur. J.* **2007**, *13*, 4197–4202.
14. Bagwe, R. P.; Hilliard, L. R.; Tan, W. Surface Modification of Silica Nanoparticles to Reduce Aggregation and Nonspecific Binding. *Langmuir* **2006**, *22*, 4357–4362.
15. Hanus, L. H.; Sooklal, K.; Murphy, C. J.; Ploehn, H. J. Aggregation Kinetics of Dendrimer-Stabilized CdS Nanoclusters. *Langmuir* **2000**, *16*, 2621–2626.
16. Breus, V. V.; Heyes, C. D.; Tron, K.; Nienhaus, G. U. Zwitterionic Biocompatible Quantum Dots for Wide pH Stability and Weak Nonspecific Binding to Cells. *ACS Nano* **2009**, *3*, 2573–2580.
17. Yu, W. W.; Chang, E.; Falkner, J. C.; Zhang, J.; Al-Somali, A. M.; Sayes, C. M.; Johns, J.; Drezek, R.; Colvin, V. L. Forming Biocompatible and Nonaggregated Nanocrystals in Water Using Amphiphilic Polymers. *J. Am. Chem. Soc.* **2007**, *129*, 2871–2879.
18. Bentzen, E. L.; Tomlinson, I. D.; Mason, J.; Gresch, P.; Warnement, M. R.; Wright, D.; Sanders-Bush, E.; Blakely, R.; Rosenthal, S. J. Surface Modification To Reduce Nonspecific Binding of Quantum Dots in Live Cell Assays. *Bioconjugate Chem.* **2005**, *16*, 1488–1494.
19. Stewart, M. H.; Susumu, K.; Mei, B. C.; Medintz, I. L.; Delehanty, J. B.; Blanco-Canosa, J. B.; Dawson, P. E.; Mattoussi, H. Multidentate Poly(ethylene glycol) Ligands Provide Colloidal Stability to Semiconductor and Metallic Nanocrystals in Extreme Conditions. *J. Am. Chem. Soc.* **2010**, *132*, 9804–9813.
20. Pellegrino, T.; Manna, L.; Kudera, S.; Liedl, T.; Koktysh, D.; Rogach, A. L.; Keller, S.; Rdler, J.; Natile, G.; Parak, W. J. Hydrophobic Nanocrystals Coated with an Amphiphilic Polymer Shell: A General Route to Water Soluble Nanocrystals. *Nano Lett.* **2004**, *4*, 703–707.

21. Lees, E. E.; Nguyen, T. L.; Clayton, A. H. A.; Mulvaney, P. The Preparation of Colloidally Stable, Water-Soluble, Biocompatible, Semiconductor Nanocrystals with a Small Hydrodynamic Diameter. *ACS Nano* **2009**, *3*, 1121–1128.
22. Kairdolf, B. A.; Mancini, M. C.; Smith, A. M.; Nie, S. Minimizing Nonspecific Cellular Binding of Quantum Dots with Hydroxyl-Derivatized Surface Coatings. *Anal. Chem.* **2008**, *80*, 3029–3034.
23. Dubertret, B.; Skourides, P.; Norris, D. J.; Noireaux, V.; Brivanlou, A. H.; Libchaber, A. *In Vivo* Imaging of Quantum Dots Encapsulated in Phospholipid Micelles. *Science* **2002**, *298*, 1759–1762.
24. Wang, Y. A.; Li, J. J.; Chen, H.; Peng, X. Stabilization of Inorganic Nanocrystals by Organic Dendrons. *J. Am. Chem. Soc.* **2002**, *124*, 2293–2298.
25. Kim, S.; Bawendi, M. G. Oligomeric Ligands for Luminescent and Stable Nanocrystal Quantum Dots. *J. Am. Chem. Soc.* **2003**, *125*, 14652–14653.
26. Haviv, A. H.; Greneche, J. M.; Lellouche, J. P. Aggregation Control of Hydrophilic Maghemite (gamma-Fe_2O_3) Nanoparticles by Surface Doping Using Cerium Atoms. *J. Am. Chem. Soc.* **2010**, *132*, 12519–12521.
27. Yee, C.; Kataby, G.; Ulman, A.; Prozorov, T.; White, H.; King, A.; Rafailovich, M.; Sokolov, J.; Gedanken, A. Self-Assembled Monolayers of Alkanesulfonic and -Phosphonic Acids on Amorphous Iron Oxide Nanoparticles. *Langmuir* **1999**, *15*, 7111–7115.
28. Sistach, S. p.; Rahme, K.; Prignon, N.; Marty, J. D.; Viguerie, N. L.; Gauffre, F.; Mingotaud, C. Bolaamphiphile Surfactants as Nanoparticle Stabilizers: Application to Reversible Aggregation of Gold Nanoparticles. *Chem. Mater.* **2008**, *20*, 1221–1223.
29. Sharma, K. P.; Aswal, V. K.; Kumaraswamy, G. Adsorption of Nonionic Surfactant on Silica Nanoparticles: Structure and Resultant Interparticle Interactions. *J Phy. Chem. B* **2010**, *114*, 10986–10994.
30. Poderys, V.; Matulionyte, M.; Selskis, A.; Rotomskis, R. Interaction of Water-Soluble CdTe Quantum Dots with Bovine Serum Albumin. *Nanoscale Res. Lett.* **2011**, *6*, 9.
31. Kaul, Z.; Yaguchi, T.; Kaul, S. C.; Hirano, T.; Wadhwa, R.; Taira, K. Mortalin Imaging in Normal and Cancer Cells with Quantum Dot Immuno-conjugates. *Cell Res.* **2003**, *13*, 503–507.
32. Kim, T.; Noh, M.; Lee, H.; Joo, S. W.; Lee, S. Y.; Lee, K. Fluorescence-Based Detection of Point Mutation in DNA Sequences by CdS Quantum Dot Aggregation. *J. Phys. Chem. B* **2009**, *113*, 14487–14490.
33. Sharma, K. P.; Aswal, V. K.; Kumaraswamy, G. Adsorption of Nonionic Surfactant on Silica Nanoparticles: Structure and Resultant Interparticle Interactions. *J. Phys. Chem. B* **2010**, *114*, 10986–10994.
34. Liu, J.; Yang, X.; Wang, K.; Yang, R.; Ji, H.; Yang, L.; Wu, C. A Switchable Fluorescent Quantum Dot Probe Based on Aggregation/Disaggregation Mechanism. *Chem. Commun.* **2011**, *47*, 935–937.
35. Emsley, J. Very Strong Hydrogen Bonding. *Chem. Soc. Rev.* **1980**, *9*, 91–124.
36. Teng, M.; Kuang, G.; Jia, X.; Gao, M.; Li, Y.; Wei, Y. Glycine−Glutamic-Acid-Based Organogelators and Their Fluoride Anion Responsive Properties. *J. Mater. Chem.* **2009**, *19*, 5648–5654.
37. Kim, T. H.; Kwon, N. Y.; Lee, T. S. Synthesis of Organogelling, Fluoride Ion-Responsive, Cholesteryl-Based Benzoxazole Containing Intra- and Intermolecular Hydrogen-Bonding Sites. *Tetrahedron Lett.* **2010**, *51*, 5596–5600.
38. Yang, W. H.; Li, W. W.; Dou, H. J.; Sun, K. Hydrothermal Synthesis for High-Quality CdTe Quantum Dots Capped by Cysteamine. *Mater. Lett.* **2008**, *62*, 2564–2566.
39. Lee, C.; Jang, D.; Cheong, S.; Kim, E.; Jeong, M.; Kim, S.; Kim, D.; Lim, S. T.; Sohn, M.; Jeong, H. Surface Engineering of Quantum Dots for *in Vivo* Imaging. *Nanotechnology* **2010**, *21*, 285102.
40. Gaponik, N.; Talapin, D. V.; Rogach, A. L.; Hoppe, K.; Shevchenko, E. V.; Kornowski, A.; Eychmller, A.; Weller, H. Thiol-Capping of CdTe Nanocrystals: An Alternative to Organometallic Synthetic Routes. *J. Phys. Chem. B* **2002**, *106*, 7177–7185.
41. Joonhyuck, P.; Jutaek, N.; Nayoun, W.; Ho, J.; Sungho, J.; Sungwook, J.; So-Hye, C.; Sungjee, K. Compact and Stable Quantum Dots with Positive, Negative, or Zwitterionic Surface: Specific Cell Interactions and Non-specific Adsorptions by the Surface Charges. *Adv. Funct. Mater.* **2011**, *21*, 1558–1566.
42. Soo Choi, H.; Liu, W.; Misra, P.; Tanaka, E.; Zimmer, J. P.; Itty Ipe, B.; Bawendi, M. G.; Frangioni, J. V. Renal Clearance of Quantum Dots. *Nat. Biotechnol.* **2007**, *25*, 1165–1170.
43. Camargo, J. A. Fluoride Toxicity to Aquatic Organisms: A Review. *Chemosphere* **2003**, *50*, 251–264.
44. Ayoob, S.; Gupta, A. K. Fluoride in Drinking Water: A Review on the Status and Stress Effects. *Crit. Rev. Env. Sci. Technol.* **2006**, *36*, 433–487.
45. Li, C.; Zhu, Y. Y.; Yi, H. P.; Li, C. Z.; Jiang, X. K.; Li, Z. T.; Yu, Y. H. Strong Stacking between F−HN Hydrogen-Bonded Foldamers and Fullerenes: Formation of Supramolecular Nano Networks. *Chem.—Eur. J.* **2007**, *13*, 9990–9998.
46. Olah, G. A.; Mathew, T.; Goeppert, A.; Trk, B.; Bucsi, I.; Li, X. Y.; Wang, Q.; Marinez, E. R.; Batamack, P.; Aniszfeld, R.; Prakash, G. K. S. Ionic Liquid and Solid HF Equivalent Amine-Poly(hydrogen fluoride) Complexes Effecting Efficient Environmentally Friendly Isobutane Isobutylene Alkylation. *J. Am. Chem. Soc.* **2005**, *127*, 5964–5969.
47. Koole, R.; Liljeroth, P.; de Mello Doneg, C.; Vanmaekelbergh, D. I.; Meijerink, A. Electronic Coupling and Exciton Energy Transfer in CdTe Quantum-Dot Molecules. *J. Am. Chem. Soc.* **2006**, *128*, 10436–10441.
48. Wu, M.; Mukherjee, P.; Lamont, D. N.; Waldeck, D. H. Electron Transfer and Fluorescence Quenching of Nanoparticle Assemblies. *J. Phys. Chem. C* **2010**, *114*, 5751–5759.
49. Wu, W.; Zhou, T.; Berliner, A.; Banerjee, P.; Zhou, S. Glucose-Mediated Assembly of Phenylboronic Acid Modified CdTe/ZnTe/ZnS Quantum Dots for Intracellular Glucose Probing. *Angew. Chem., Int. Ed.* **2010**, *49*, 6554–6558.
50. Knappenberger, K. L.; Wong, D. B.; Romanyuk, Y. E.; Leone, S. R. Excitation Wavelength Dependence of Fluorescence Intermittency in CdSe/ZnS Core/Shell Quantum Dots. *Nano Lett.* **2007**, *7*, 3869–3874.
51. Nirmal, M.; Dabbousi, B. O.; Bawendi, M. G.; Macklin, J. J.; Trautman, J. K.; Harris, T. D.; Brus, L. E. Fluorescence Intermittency in Single Cadmium Selenide Nanocrystals. *Nature* **1996**, *383*, 802–804.
52. Chen, Y.; Vela, J.; Htoon, H.; Casson, J. L.; Werder, D. J.; Bussian, D. A.; Klimov, V. I.; Hollingsworth, J. A. "Giant" Multishell CdSe Nanocrystal Quantum Dots with Suppressed Blinking. *J. Am. Chem. Soc.* **2008**, *130*, 5026–5027.
53. Golubev, N. S.; Tolstoy, P. M.; Smirnov, S. N.; Denisov, G. S.; Limbach, H. H. Low-Temperature NMR Spectra of Fluoride-Acetic Acid Hydrogen-Bonded Complexes in Aprotic Polar Environment. *J. Mol. Struct.* **2004**, *700*, 3–12.
54. John, A. *Dean Lange's Handbook of Chemistry*, 15th ed.; McGraw-Hill Professional: New York, 1998.
55. Biswas, K.; Saha, S. K.; Ghosh, U. C. Adsorption of Fluoride from Aqueous Solution by a Synthetic Iron(III)−Aluminum(III) Mixed Oxide. *Ind. Eng. Chem. Res.* **2007**, *46*, 5346–5356.
56. Bhatnagar, A.; Kumar, E.; Sillanp, M. Fluoride Removal from Water by Adsorption: A Review. *Chem. Eng. J.* **2011**, *171*, 811–840.
57. Medellin-Castillo, N. A.; Leyva-Ramos, R.; Ocampo-Perez, R.; Garcia de la Cruz, R.; ragon-Pia, A.; Martinez-Rosales, J. M.; Guerrero-Coronado, R. M.; Fuentes-Rubio, L. Adsorption of Fluoride from Water Solution on Bone Char. *Ind. Eng. Chem. Res.* **2007**, *46*, 9205–9212.
58. Batistella, L.; Venquiaruto, L. D.; Di Luccio, M.; Oliveira, J. V.; Pergher, S. B. C.; Mazutti, M. A.; de Oliveira, D. b.; Mossi, A. J.; Treichel, H.; Dallago, R. Evaluation of Acid Activation under the Adsorption Capacity of Double Layered Hydroxides of Mg−Al−CO_3 Type for Fluoride Removal from Aqueous Medium. *Ind. Eng. Chem. Res.* **2011**, *50*, 6871–6876.
59. Lide, D. R. *CRC Handbook of Chemistry and Physics*, 84th ed.; Chapman & Hall/CRC Press: Boca Raton, FL, 2004.

60. Zhang, X. F.; Yang, S. H. Nonspecific Adsorption of Charged Quantum Dots on Supported Zwitterionic Lipid Bilayers: Real-Time Monitoring by Quartz Crystal Microbalance with Dissipation. *Langmuir* **2011**, *27*, 2528–2535.
61. Khalil, A. M.; Da'dara, A. A. The Genotoxic and Cytotoxic Activities of Inorganic Fluoride in Cultured Rat Bone Marrow Cells. *Arch. Environ. Contam. Toxicol.* **1994**, *26*, 60–63.
62. Yu, W. W.; Qu, L.; Guo, W.; Peng, X. Experimental Determination of the Extinction Coefficient of CdTe, CdSe, and CdS Nanocrystals. *Chem. Mater.* **2003**, *15*, 2854–2860.